Supplementary Materials for

Human α-defensin 6 promotes mucosal innate immunity through self-assembled peptide nanonets

Hiutung Chu, Marzena Pazgier, Grace Jung, Sean-Paul Nuccio, Patricia A. Castillo, Maarten F. de Jong, Maria G. Winter, Sebastian E. Winter, Jan Wehkamp, Bo Shen, Nita H. Salzman, Mark A. Underwood, Renee M. Tsolis, Glenn M. Young, Wuyuan Lu, Robert I. Lehrer, Andreas J. Bäumler and Charles L. Bevins

Correspondence to: clbevins@ucdavis.edu

This PDF file includes:

Materials and Methods

Ethics Approval

The Institutional Animal Care and Use Committee at the University of California, Davis, approved the animal experiments. The Cleveland Clinic Institutional Review Board approved the protocol for obtaining ileal aspirates for this study (#06-673) and informed consent was obtained from all patients.

Peptides

All peptides (HD6, HD5, H27W-HD6, Cryptdin-2, and Cryptdin-3) used were synthetically prepared, purified and characterized to confirm proper mass and disulfide connectivity, as previously described (*15*).

Generation of HD6 transgenic mice

A 3.34 kb fragment of the genomic sequence containing the HD6 gene, including 1.47 kb of the 5' flanking region, was used as the transgene in the generation of transgenic mice modeled after a previously described approach (*7*). Briefly, an EcoRV-EcoRI restriction fragment from a recombinant lambda phage clone containing the HD6 gene (*25*) was isolated and subcloned into a bacterial plasmid and sequenced in its entirety. The EcoRV-EcoRI plasmid insert was then isolated, purified, and microinjected into fertilized FVB mouse oocytes, which were then transplanted into pseudopregnant FVB mice by the UC Davis Mouse Biology Program Transgenic core facility. Genomic DNA isolated from the tails of potential founder mouse pups was analyzed by PCR using HD6-specific

oligonucleotide primers, HD6-79s (CCACTCCAAGCTGAGGAT) and HD6-183a (CTCTGCAAAGGAGACGGC). A founder mouse expressing the HD6 transgene was identified, bred with a wild-type FVB mouse to generate hemizygous offspring, and create a transgenic line for study.

Western blot analysis

Protein extracts from human and mouse tissues were isolated as previously described (*23*), with some minor modifications. Briefly, approximately 1 g of tissue was homogenized with a Brinkmann Polytron homogenizer in ice-cold 20% acetic acid (1:10 w/v) that contained 1:100 (v/v) Protease Inhibitor Cocktail III (Calbiochem, La Jolla, CA). The extracts were stirred overnight in 4ºC and clarified the following day by ultracentrifugation (110,000 X g at 4ºC for 30 min). AU-PAGE was performed on the tissue extracts, as described (*23*). Briefly, samples were analyzed on 12.5% acrylamide/2% bis-acrylamide (Roche Diagnostics, Indianapolis, IN), 8 M deionized urea, and 5% acetic acid gels. Proteins were transferred to Immobilon P^{SQ} PVDF membrane (Millipore, Billerica, MA) in 5% acetic acid using a semi-dry transfer apparatus (Fisher Scientific, Pittsburgh, PA) at 1.5 mA/cm^2 reverse polarity (transfer driven to cathode) for 20 min. The membrane was then fixed with 0.01% glutaraldehyde (Sigma, St. Louis, MO) for 15 min, washed in Tris-buffered saline, and blocked in 5% nonfat dry milk for 1 h. The blots were probed with α-HD6 (1:3500) or α-human lysozyme (1:1000) (Dako Cytomation, Denmark) rabbit polyclonal antibodies using a horseradish peroxidase (HRP)-conjugated goat α-rabbit secondary antibody (KPL, Gaithersburg, Maryland) and developed using Immobilon Western chemiluminescent

HRP substrate (Millipore, Billerica, MA). Chemiluminescent signal was detected with a Biospectrum AC Imaging System (UVP, Upland, CA)

Immunohistochemistry

Distal ileal tissue was dissected, immediately fixed in 4% paraformaldehyde overnight, and then dehydrated in graded-ethanol before embedding in paraffin blocks. Sections (4 μm) were cut, deparaffinized, rehydrated in graded ethanol, treated with peroxide and washed in PBS. The sections were blocked with 5% goat serum and incubated with rabbit αHD6 (1:19,000 in 5% goat serum in phosphate-buffered saline (PBS)) overnight at 4ºC in a humidified chamber. Sections were then washed in PBS, blocked with 5% goat serum, and incubated with biotinylated goat anti-rabbit (1:200) (Vector Laboratories, Burlingame, CA) for 20 min, followed by treatment with HRP-conjugated avidin-biotin complex (Vector Laboratories, Burlingame, CA). The sections were washed and incubated with 3,3' diaminobenzidine (DAB) substrate (Vector Laboratories, Burlingame, CA) for 5 min at room temperature, followed by light green counterstain.

RNA isolation and reverse transcription

Tissue samples were harvested, incubated in RNA*later* (Ambion, Foster City, CA) overnight at room temperature, and then frozen and stored in -80ºC. Frozen specimens were thawed and immediately homogenized in guanidine thiocyanate buffer. Total RNA was isolated using cesium chloride gradient ultracentrifugation, as previously described (*26*). RNA was reverse transcribed using Superscript II reverse transcriptase (Invitrogen, Carlsbad, CA) (*26*) and corresponding cDNA was purified using Qiagen PCR

purification kit (Qiagen, Valencia, CA) and diluted to 10 ng/µl based on the input concentration of total RNA.

Quantitative real-time RT-PCR of Paneth cell products

Gene-specific primers were designed using MacVector software (MacVector, Cary, NC) and synthesized by Invitrogen Life Technologies (Invitrogen, Carlsbad, CA). Real-time PCR was performed on tissue-specific cDNA as a template using the LightCycler 2.0 (Roche Diagnostics, Indianapolis, IN), as previously described (*26*). Absolute quantification was performed using gene-specific external standards within each run.

Bacterial strains

Bacterial strains are listed in Table S1. Cultures of *S.* Typhimurium were incubated aerobically at 37°C in Luria-Bertani (LB) broth (per liter: 10 g tryptone, 5 g yeast extract, 10 g NaCl) or on LB agar plates (1.5% Difco agar) overnight. The strain of S. Typhimurium (IR715) is a nalidixic acid-resistant strain of 14028. Nalidixic acid was added at 50 mg/L. Cultures of *Y. enterocolitica* (GY123 and GY5583) were grown aerobically at 23ºC in LB broth and agar plates. Cultures of *C. rodentium* (*ATCC* 51459) and *E. coli* were incubated aerobically at 37ºC in LB broth and agar plates.

Strain construction

The Δ*fim*::KSAC deletion of *S.* Typhimurium strain EHW2 was introduced into SPN313 by generalized transduction with a bacteriophage P22 HT105/1 *int*-201 lysate of EHW2, selecting for kanamycin resistance (100µg/mL Luria Bertani agar) of SPN313

transductants. Transductants were purified from phage on Evans blue uridine agar verified to be sensitive to P22 H5 lysis, and deletion of *fimAICDHF* by the KSAC cassette was confirmed by PCR with oligonucleotide primer pairs directed to KSAC (Genbank accession V00359.1) and regions up and downstream of the *S.* Typhimurium *fim* operon (Genbank accession AE006468.1): KSAC5'out (GGCATAAATTCCGTCAGC) and FIMdown (GCACTTATCCTGTTGACC), KSAC3'out (TGATGACGAGCGTAATGG) and FIMup (CGTCTACGTCTTTATCTGG). Loss of *fimA* was confirmed by PCR with oligonucleotide primers FIMA1 (GCTGATCCTACTCCGGTG) and FIMA2 (AAAATGGAACGCTGACGGGAGC). A transductant meeting these criteria was designated SPN494.

Antimicrobial Assay

Radial diffusion assays were performed with *S.* Typhimurium (IR715), *Y. enterocolitica* (GY123), and *E. coli* D31, as previously described (*27*), using either 10 μg HD5 or 10 μg HD6. Briefly, bacteria were grown aerobically, pelleted, washed and resuspended with 10 mM sodium phosphate buffer, pH 7.4. 4 x 10^6 CFU bacteria were inoculated into warm 1% (wt/vol) low electroendosmosis (EEO) agarose (Sigma) and poured into a polystyrene culture dish. A well (3 mm diameter) was punched into the solidified agarose layer. Defensin peptide (HD6 or HD5) was then added into the wells and allowed to diffuse into the agarose for 3 h at 37ºC. The plate was then overlaid with 6% TSB with 1% low EEO agarose. After overnight incubation at 37ºC, clear zones of bacterial killing surrounding each well were measured.

Salmonella-infection of HD6 transgenic animals

Female FVB HD6 hemizygous mice and wild-type littermates (6 – 8 weeks of age) were intragastrically infected with 2 x 10^8 CFU *S.* Typhimurium IR715. *S.* Typhimurium were grown aerobically at 37ºC for 18 h in LB broth. Mice were euthanized 4 or 6 days after bacterial inoculation, and the Peyer's patches (three per animal), spleen, and fecal pellets were harvested for bacterial colony counts. Thus, tissues were homogenized in PBS and serially diluted ten-fold and plated on LB agar plates containing nalidixic acid (50 mg/L) for bacterial enumeration.

To address the issue of bacterial aggregation, we performed control experiments using known amounts of S. Typhimurium and added 10 μg/ml HD6 to induce aggregation. We then vortexed the sample, serially diluted aliquots and plated the bacteria. The CFU output was identical to the input amount (within experimental variability). Similarly, tissues were homogenized using a polytron at a speed of 24,000 rpm, which also breaks up bacterial aggregates.

In vitro invasion assay

The human cell lines T84 (ATCC CCL-248) and INT-407 (ATCC CCL-6), and mouse small intestinal cell line MODE-K (*28*) were cultured in Dulbecco modified Eagle medium/F12 (DMEM/F12, Invitrogen, Carlsbad, CA) and Dulbecco modified Eagle medium (DMEM, Invitrogen, Carlsbad, CA), respectively in 24-well plates at a density of ~10^5 cells per well as described (*29*). *S.* Typhimurium (1 x 10^6 CFU) were treated for

30 min with 10 μg/ml peptide (HD5, HD6 or H27W-HD6) in a final volume of 500 μl media at room temperature. The epithelial cells were then infected with α-defensin pretreated (or vehicle-treated control) *S.* Typhimurium (MOI of 10) at 37ºC in media and an atmosphere of 5% CO_2. After 1 h of infection, the media was aspirated, and the cells were washed with PBS. The cells were then treated with 100 μg/ml of gentamicin (Invitrogen, Carlsbad, CA) in DMEM/F12 for 1.5 h at 37ºC in 5% CO_2 to kill extracellular bacteria. Cells were washed once more with PBS, and then lysed with 0.05% Triton X-100. Bacterial numbers were determined by plating on selective media. Adhesion assays were performed as described above, except that gentamicin was omitted.

Immunofluorescence microscopy

S. Typhimurium expressing Green Fluorescent Protein (GFP) was treated with α-defensin peptide (10 μg/ml) and then added to culture of T84 cells grown on glass coverslips, using the invasion protocol described above. After the cells were washed with PBS, treated with 100 μg/ml of gentamicin (Invitrogen, Carlsbad, CA), and washed again in PBS, they were fixed with 3% paraformaldehyde in PBS at 37ºC for 10 min. The fixed cells were washed with PBS and blocked with 10% goat serum in PBS for 30 min at room temperature. Coverslips were inverted onto a solution of 1:1000 αLPS (Difco, Sparks, MD) and incubated at room temperature in a humidified chamber for 1 h. The coverslips were washed with PBS and inverted onto a solution of 1:500 Alexa Fluor 568 secondary anti-rabbit antibody (Invitrogen Molecular Probes, Carlsbad, CA) for 1 h in a humidified chamber, in darkness. Cells were washed twice in PBS, and once in water and

then mounted with Mowiol 4-88 (Calbiochem, Gibbstown, NJ) containing DAPI onto glass slides and visualize on Zeiss confocal microscope.

Bacterial RNA Isolation

Bacterial RNA was isolated using the Aurum Total RNA Kit (Bio-Rad Laboratories, Hercules, CA) according to the recommendations of the manufacturer. RT-PCR and quantitative RT- PCR were performed as described previously (*30*). The comparative Ct method was used to analyze the data. Levels of *flhD*, *fliC*, *hilA*, and *invG* mRNA in each sample were normalized to the respective levels of *RpoD* mRNA, encoded by the *rpoD* gene.

Isolation of genomic DNA from stool

Stool pellets were isolated from distal colon of mice and stored in RNAlater (Ambion, Foster City, CA) (*9*). Samples were thawed, weighed, washed in ice-cold PBS, and resuspended in 20 mM Tris-HCl, pH 8.0, 2 mM EDTA, 1.2% Triton X-100, and 40 µg/ml lysozyme (Sigma, St. Louis, MO). Samples were then transferred to a screw cap tube containing zirconium beads (MP Biomedicals, Irvine, CA) and incubated at 37^{o}C for 30 min. Buffer ASL (Qiagen, Valencia, CA) was added to the mixture and the sample was subjected to bead beating (BioSpec, Bartlesville, OK) for 2 min at maximum speed (6.5 m/s). The resulting suspension was incubated at 95^{o}C for 5 min and genomic DNA was then isolated with the Qiagen Stool Kit (Qiagen, Valencia, CA) according to manufacturer's protocol.

Quantitative real-time PCR analysis of fecal microbiota

Group-specific 16S rDNA primers were used in quantitative real-time PCR to measure the abundance of bacterial groups in mouse intestine using isolated genomic DNA as described (*9*).

Surface Plasmon Resonance

Surface plasmon resonance studies were performed at 25°C on a BIACORE 3000 instrument (Biacore, GE Healthcare). Amine coupling was used to ligate the proteins of interest to individual flow cells on a CM5 sensor chip. The running buffer, HBS-EP (pH 7.4) contained: 10 mM HEPES, 150 mM NaCl, 3 mM EDTA, and a submicellar concentration (0.005%) of surfactant P20. Single cycle experiments were performed as previously described (*20*), with an analyte flow rate of 50 µl/min. In multi-cycle experiments, binding was measured at a flow rate of 20 µl/min for 12.5 min in each cycle. This was followed by a 2.5 min interval during which the flow cells were perfused by analyte-free HBS-EP until the sample loop had acquired the next 250 µl aliquot of analyte solution. The final analyte injection was in "kinetic mode", with a 10 min dissociation period. Molar ratios were calculated as described previously (*20*).

Recombinant, full-length, glycosylated gp120 from HIV-1(LAV) that was produced in insect cells was purchased Protein Science Corp. (Meriden, CT). It was deglycosylated in situ after affixing it to a CM5 biosensor chip. The following recombinant enzymes, all produced in *E. coli*, were purchased from Prozyme (San Leandro, CA): Sialidase A™ from *Arthrobacter ureafaciens*; *O*-Glycanase (endo-α-*N*-acetylgalactosaminidase) from

Streptococcus pneumoniae; and PNGase F (*N*-glycanase) from *Chryseobacterium meningosepticum*. The deglycosylation procedure had three steps, each lasting 3h at 37^{o}C, during which the specified enzymes were delivered at a flow rate of 2 µl/min in 50mM sodium phosphate, pH 7.0. In Steps 1 and 2, the immobilized gp120 (8213 RU) was exposed first to 50 mU/ml of Sialidase A and then to 12.5 mU/ml of *O*-glycanase. In Step 3, it was exposed for 3h to a mixture of 50 mU/ml Sialidase A, 12.5 mU/ml of *O*-Glycanase and 50 mU/ml of PNGase F.

The binding of three lectins was measured before and after the deglycosylation procedure. HHL (*Hippeastrum* hybrid lectin) detects α-(1-3,6) mannose, GNA (*Galanus nivalis* lectin) detects α 1-3 and α 1-6 linked high mannose structures, and WGA (wheat germ agglutinin) detects *N*-acetylglucosamines (GlcNAcβ1-4 GlcNAc β1-4GlcNAc) and sialic acid. In the experiment shown, before its enzymatic deglycosylation the native gp120 (8213 RU) bound 6750 RU of HHL, 6800 RU of GNA and 4720 RU of WGA. After glycosylation, it bound 2804 RU of HHL, 2455 RU of GNA and 460 RU of WGA. In addition, the density (RU) of the gp120 biosensor decreased from 8213 RU to 7115 RU, reflecting its decreased mass after carbohydrate residues had been removed.

In vitro HD6 nanonet and scanning electron microscopy

S. Typhimurium were grown to mid-logarithmic phase in LB broth. 2 x 10^6 CFU of *S.* Typhimurium in growth medium were centrifuged (5,000 x g for 5 min) and resuspended in 1 ml of 50 mM Tris-maleate buffer, pH 6.4. Bacteria were then incubated with 10 µg/ml of HD6 for 30 min at room temperature and then centrifuged (5,000 x g for 5 min)

to pellet. The bacterial pellets were then resuspended in Karnovsky's fixative (2% paraformaldehyde, 2.5% glutaraldehyde in 0.06M Sorensen's phosphate buffer (0.2 M sodium phosphate, pH 7.2)) and left overnight at room temperature. Specimens were then dehydrated in graded ethanol (twice in 95% and 100% for 15 min each) and then transferred to a critical point dryer (PELCO CPD-2) and dried with CO_2. The samples were then mounted onto 12 mm aluminum stubs followed by sputter coating with gold. Samples were photographed using a Philips XL-30 scanning electron microscope at 20 kV.

Protein A coated polystyrene beads (Spherotech, Lake Forest, IL) were treated with 1 μg/ml of HD6 or vehicle for 5 min in 50 mM Tris-maleate buffer, pH 6.4. The treated beads were then fixed in Karnovsky's fixative overnight at room temperature and processed for scanning electron microscopy, as described above. Protein from type I fimbae isolated from *S*. Typhimurium was covalently coupled to carboxylate-modified latex beads (Invitrogen, Carlsbad, CA) using manufacturer's protocols. The washed beads were then treated with HD6 and analyzed as described for the Protein A beads.

In vivo HD6 nanonet detection

Mice were anesthetized with inhaled isofurane. A 4 cm distal ileal loop was surgically exposed and ligated, as described (*19*). Pilocarpine (Tocris, Ellisville, MD) was administered intraperitoneally (1 mg/1 kg). After 30 min the mice were euthanized by overdose of isofurane and cervical dislocation. Ileal loops were then injected with 1×10^9 CFU *S*. Typhimurium. After 1 h, Karnovsky's fixative was injected into the loop and the

entire ileal loop was fixed overnight and processed for scanning electron microscopy, as described above.

Twenty images of WT or HD6 ileal loops were first scored by four individuals (PAC, RMT, AJB, and CLB) unaware of the group assignments. The presence or absence of nanonets was scored and found to be 100% concordant with genotype assignment (80 of 80 images). Next, representative images were selected by a blinded individual (PAC) and the images were evaluate by three individuals (RMT, AJB, and CLB) unaware of the genotype. The presence or absence of nanonets was again 100% concordant with genotype (36 of 36 images).

Human small intestinal fluid aspirates

Aspirates were obtained from healthy individuals who were undergoing routine screening colonoscopy for colon polyps. In preparation on the night before colonoscopy, patients were administered a routine polyethylene glycol-electrolyte solution to purge the bowel of contents, and the patients remained on clear fluids until the procedure was completed. Colonoscopy was performed in the morning, and the terminal ileum was intubated. Approximately 5-15 ml of ileal lumenal fluid was aspirated and immediately placed on dry ice. The specimen was then stored in a freezer at -80^{o}C until used for the analysis. On the day of the experiment, the fluid was thawed on wet ice and clarified by ultracentrifugation (55,000 RPM for 30 min at 4^{o}C). The clarified fluid was carefully decanted and then used as the medium for *Salmonella* aggregation experiments with HD6.

Crystallization, Data collection and Structure Determination

All crystallization experiments on H27W-HD6 were performed at room temperature by the hanging-drop vapor diffusion method with commercially available crystallization matrices from Hampton (Hampton Research, Aliso Viejo, CA). The best crystals were grown when 1 μl of defensin (at 20 mg/ml in water) was mixed with 1 μl of crystallization reagent: 0.1 M imidazole, pH 6.5, 1 M sodium acetate. A single crystal was harvested with a CryoLoop (Hampton Research), briefly immersed in a cryo-solution consisting of 30% glycerol, and flash-frozen in the nitrogen steam at 100 K.

The X-ray diffraction data were collected with a Raxis-4++ image plate detector mounted on a Rigaku-MSC Micromax 7 generator (at the X-ray Crystallography Core Facility, University of Maryland, Baltimore). The crystal belonged to a space group $P2_1$ with cell dimensions a = 33.8 Å, b = 32.7 Å, c = 54.0 Å. The structure was solved by molecular replacement and the previously published coordinates of wild-type HD6 (PDB code 1ZMQ) (*15*). The final model refined to 1.95 Å resolution had an R value of 19.2% and an R_{free} value of 24.5% with good geometry and no residues in the disallowed regions. Each asymmetric unit of the crystal lattice contained four structurally independent defensin molecules, which were essentially identical to each other with Cα root mean-square deviations (RMSD) in the range of 0.3-0.9 Å for 32 residues (Figure S13). Data collection and final refinement statistics are summarized in Table S2. The coordinates and structure factors were deposited in the PDB with accession code 3QTE. Molecular

graphics were generated using Pymol (http://pymol.org), and the programs used for data processing and structure refinement were as described (*13*).

Statistical analysis

Statistical analyses were performed with Stata software (version 9.2) (StataCorp, College Station, TX) using two tailed *t*-tests to compare geometric means (Fig. 1B), or arithmetic means (Figs. 1C, 1D, S3, S4 S6), log-rank test (Fig. 1A), Mann-Whitney rank sum test (Fig. 2), and Fisher's exact test (Fig. 5). *P* values < 0.05 were considered statistically significant.

Supplementary References

1. R. I. Lehrer, C. L. Bevins, T. Ganz, in *Mucosal Immunology, 3rd Ed.,* J. Mestecky *et al.*, Eds. (Academic Press, New York, 2004), vol. 1, pp. 95-110.
7. N. H. Salzman, D. Ghosh, K. M. Huttner, Y. Paterson, C. L. Bevins, Protection against enteric salmonellosis in transgenic mice expressing a human intestinal defensin. *Nature* **422**, 522 (2003).
9. N. H. Salzman *et al.*, Enteric defensins are essential regulators of intestinal microbial ecology. *Nat Immunol* **11**, 76 (2010).
13. G. Wei *et al.*, Trp-26 imparts functional versatility to human alpha-defensin HNP1. *J Biol Chem* **285**, 16275 (2010).
15. A. Szyk *et al.*, Crystal structures of human alpha-defensins HNP4, HD5, and HD6. *Protein Sci* **15**, 2749 (2006).
19. K. Brandl, G. Plitas, B. Schnabl, R. P. DeMatteo, E. G. Pamer, MyD88-mediated signals induce the bactericidal lectin RegIII gamma and protect mice against intestinal Listeria monocytogenes infection. *J Exp Med* **204**, 1891 (2007).
20. R. I. Lehrer *et al.*, Multivalent binding of carbohydrates by the human {alpha}-defensin, HD5. *J Immunol* **183**, 480 (2009).
23. D. Ghosh *et al.*, Paneth cell trypsin is the processing enzyme for human defensin-5. *Nat Immunol* **3**, 583 (2002).
25. E. B. Mallow *et al.*, Human enteric defensins. Gene structure and developmental expression. *J Biol Chem* **271**, 4038 (1996).
26. J. Wehkamp *et al.*, Paneth cell antimicrobial peptides: Topographical distribution and quantification in gastrointestinal tissues. *FEBS Letters* **580**, 5344 (2006).
27. R. I. Lehrer, M. Rosenman, S. S. Harwig, R. Jackson, P. Eisenhauer, Ultrasensitive assays for endogenous antimicrobial polypeptides. *J Immunol Methods* **137**, 167 (1991).
28. S. M. Vidal, D. Malo, K. Vogan, E. Skamene, P. Gros, Natural resistance to infection with intracellular parasites: isolation of a candidate for Bcg. *Cell* **73**, 469 (1993).
29. S. E. Winter *et al.*, Contribution of flagellin pattern recognition to intestinal inflammation during Salmonella enterica serotype Typhimurium infection. *Infect Immun* **77**, 1904 (2009).
30. S. E. Winter *et al.*, Gut inflammation provides a respiratory electron acceptor for Salmonella. *Nature* **467**, 426 (2010).
31. I. Stojiljkovic, A. J. Baumler, F. Heffron, Ethanolamine utilization in Salmonella typhimurium: nucleotide sequence, protein expression, and mutational analysis of the cchA cchB eutE eutJ eutG eutH gene cluster. *J Bacteriol* **177**, 1357 (1995).
32. E. H. Weening *et al.*, The Salmonella enterica serotype Typhimurium lpf, bcf, stb, stc, std, and sth fimbrial operons are required for intestinal persistence in mice. *Infect Immun* **73**, 3358 (2005).
33. M. Raffatellu *et al.*, Lipocalin-2 resistance confers an advantage to Salmonella enterica serotype Typhimurium for growth and survival in the inflamed intestine. *Cell Host Microbe* **5**, 476 (2009).
34. A. T. Brunger, Free R value: a novel statistical quantity for assessing the accuracy of crystal structures. *Nature* **355**, 472 (1992).

Fig. S1

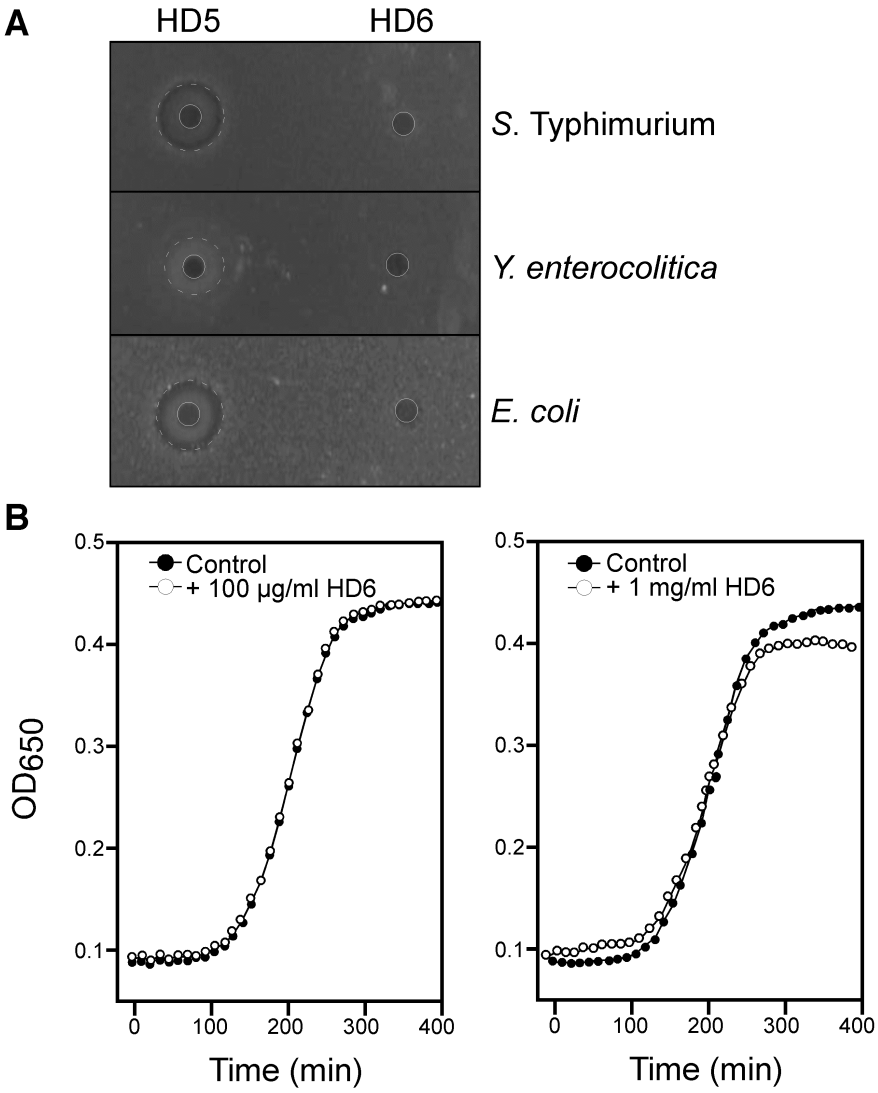

Fig. S1. Antibacterial activity of HD6.

(A) Radial diffusion assay (*27*) testing HD5 and HD6 antibacterial activity against *S*. Typhimurium (IR715), *Y. enterocolitica* (GY123), and *E. coli* D21. Wells (3 mm, solid white circles) contained 10 µg of defensin peptide. Zones of clearance in the bacterial lawns (dashed white circles) indicate bactericidal activity as previously described (*27*). See methods for description. Data are representative of six independent experiments. (B) Growth of *S.* Typhimurium monitored over time by optical density at 650 nm in liquid culture with (open circles) or without (filled circles) 100 µg/ml HD6 (left panel), or 1 mg/ml HD6 (right panel) of HD6. This experiment was performed once with the two peptide concentrations shown.

Fig. S2

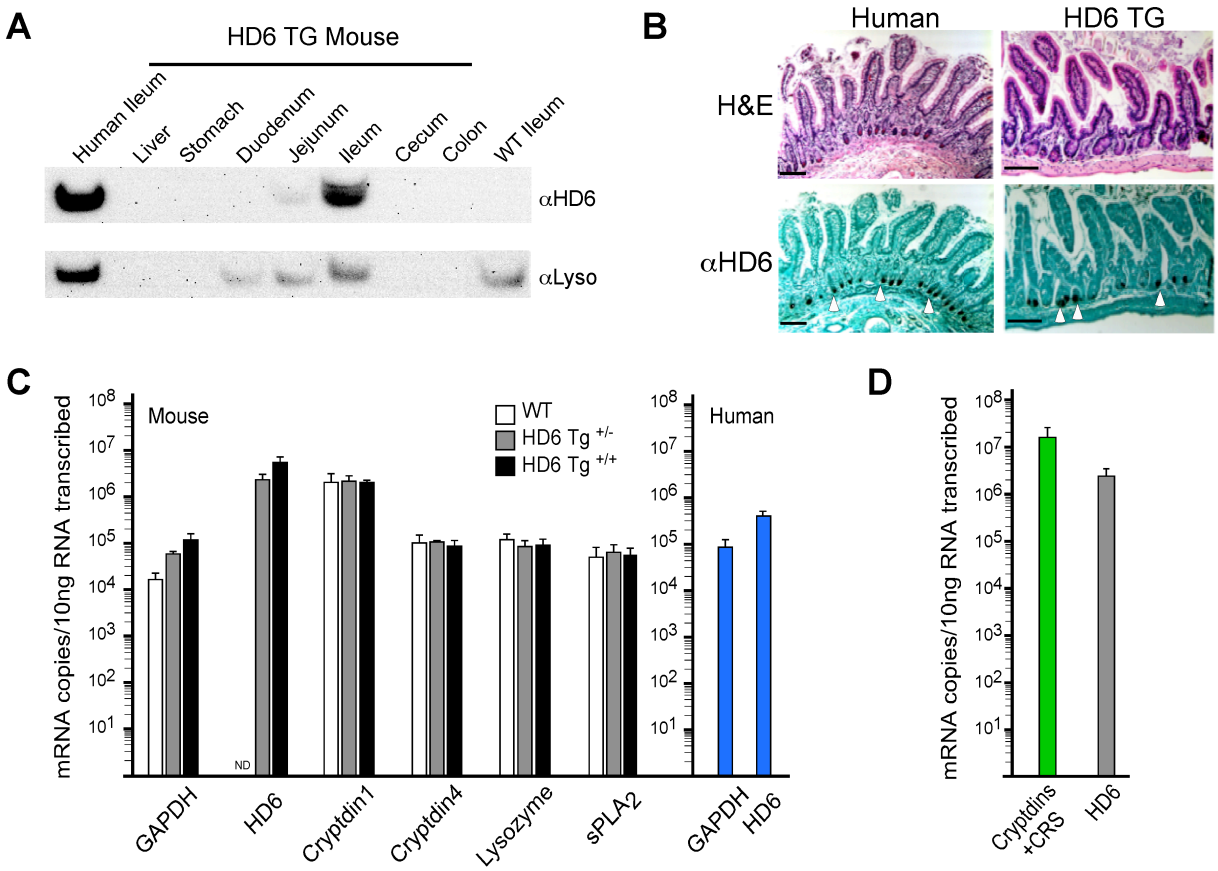

Fig. S2. Characterization of HD6 transgenic mouse.

(A) Western blot analysis of liver, stomach, duodenum, jejunum, ileum, cecum and colon from HD6 hemizygous (+/-) transgenic mice probed sequentially for HD6 and lysozyme immunoreactivity. Ileal tissue from a strain-appropriate (FVB) wild-type mouse (WT Ileum) and human (Human Ileum) served as controls. (B) Immunohistochemical analysis of human and HD6 transgenic mouse intestine. Ileal sections were stained with H&E (left) or probed with HD6 antiserum. Bar = 50 μm. Arrowheads indicate representative positive immunoreactivity in Paneth cells. (C) Quantitative real-time qPCR analysis of ileum of wild-type, hemizygous (+/-) and homozygous (+/+) HD6 transgenic mice. RNA from human ileum was analyzed as a comparator (blue). (D) Quantitative real-time RT-PCR analysis of mouse α-defensins (Cryptdins), cryptdin-related sequences (CRS), and HD6 using RNA from ileum of HD6 hemizygous (+/-) transgenic mice. A-C are data representative of four independent experiments, and D is representative of two independent experiments. Error bars are SEM.

Fig. S3

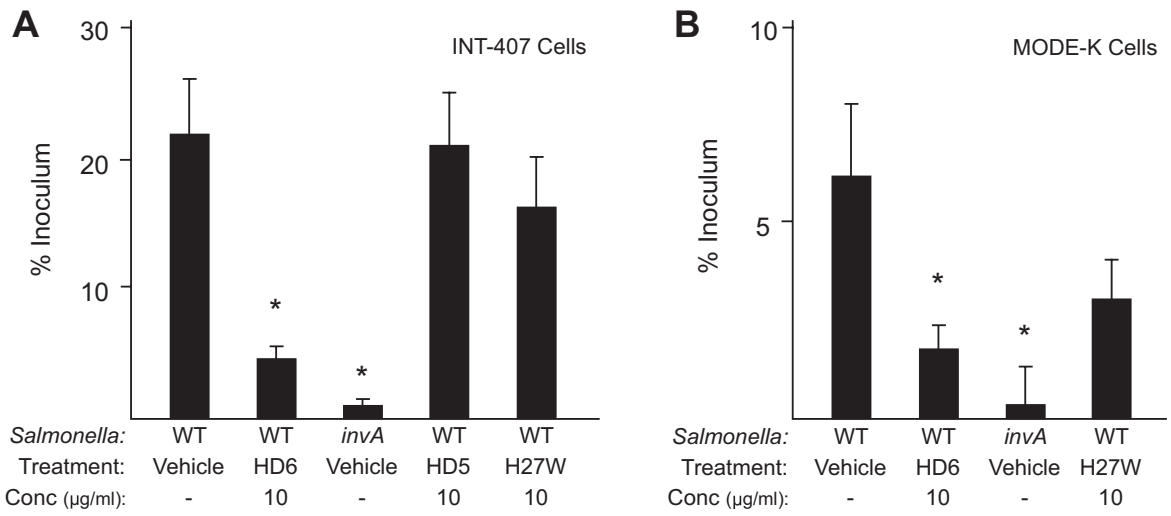

Fig. S3 HD6 inhibits *Salmonella* invasion *in vitro* of INT-407 and MODE-K cells

(A) *In vitro* invasion assay of wild-type *S.* Typhimurium using human INT-407 cells. *S.* Typhimurium were pre-treated for 1 h with either HD6, HD5, or H27W-HD6 (10 μg/ml), or with vehicle alone. Invasion-deficient *S.* Typhimurium (*invA*) were treated with vehicle alone. Bacteria were then allowed to invade the epithelial cells (MOI of 10) for 1 h. Cells were then washed, treated with gentamicin, and then lysed to quantitate intracellular bacteria (expressed as % of initial inoculum). (B) *In vitro* invasion assay of wild-type *S.* Typhimurium using mouse small intestinal MODE-K cells (MOI of 10) as described for panel A. (A-B) Data are representative of three independent experiments. Error bars represent SEM. **P* < 0.01 compared to WT vehicle, *t*- test.

Fig. S4

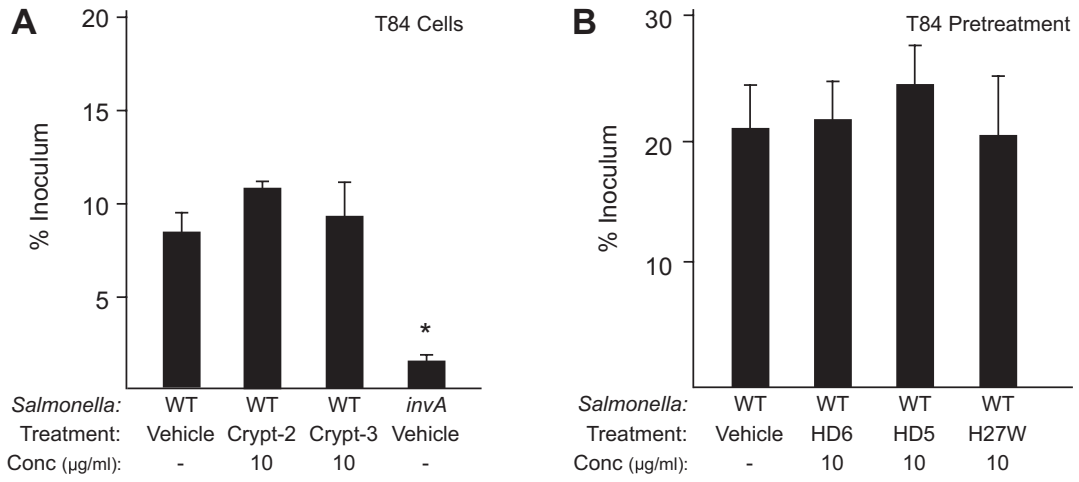

Fig. S4. *Salmonella* invasion of epithelial cells *in vitro* is not blocked by cryptdins nor by pretreatment of epithelial cells with HD6.

(A) *In vitro* invasion assay of wild-type *S.* Typhimurium using T84 cells. *S.* Typhimurium were pre-treated for 1 h with either mouse cryptdin-2 or mouse cryptdin-3 (10μg/ml), or with vehicle alone for 1 h. The *invA* mutant was treated with vehicle alone. Bacteria were then allowed to invade the epithelial cells (MOI of 10) for 1 h. Cells were then washed, treated with gentamicin, and then lysed to quantitate intracellular bacteria (expressed as % of initial inoculum). Assay conditions were identical to those used in Fig. 1, C and D. An average of three experiments is shown and are representative of nine independent experiments. (B) *In vitro* invasion assay of *S.* Typhimurium using colonic T84 cells. Epithelial cells were preincubated with vehicle alone, 10 μg/ml of HD5, HD6 or H27W HD6 for 1 h. Wild-type *S.* Typhimurium were then allowed to invade the epithelial cells (MOI of 10) for 1 h. Cells were then washed, treated with gentamicin, and then lysed to quantitate intracellular bacteria (expressed as % of initial inoculum). Note that in this experiment, the epithelial cells, not the bacteria, were pre-treated with α-defensin peptide. Data are representative of three independent experiments. Error bars represent SEM. **P* < 0.01 compared to WT vehicle, *t*- test.

Fig. S5

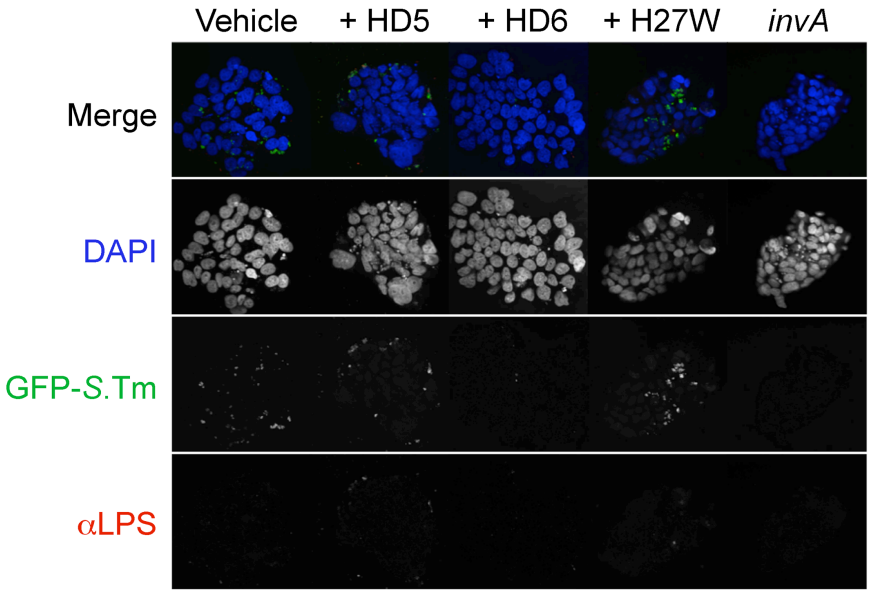

Fig. S5 Analysis of *in vitro* invasion by *S.* Typhimurium.

Confocal fluorescent microscopy of GFP-expressing *S.* Typhimurium (green) invasion of T84 cells (MOI of 60). Bacteria were pre-treated for 1 h with either vehicle alone, or with 10 μg/ml of HD5, HD6 or H27W HD6. The *invA* mutant bacteria were treated with vehicle alone. Bacteria were then allowed to invade the epithelial cells for 1 h. Cells were stained with α-LPS (red) to visualize extracellular bacteria, and DAPI (blue) to visualize nucleic acid. See methods for details. Data are representative of three independent experiments.

Fig. S6

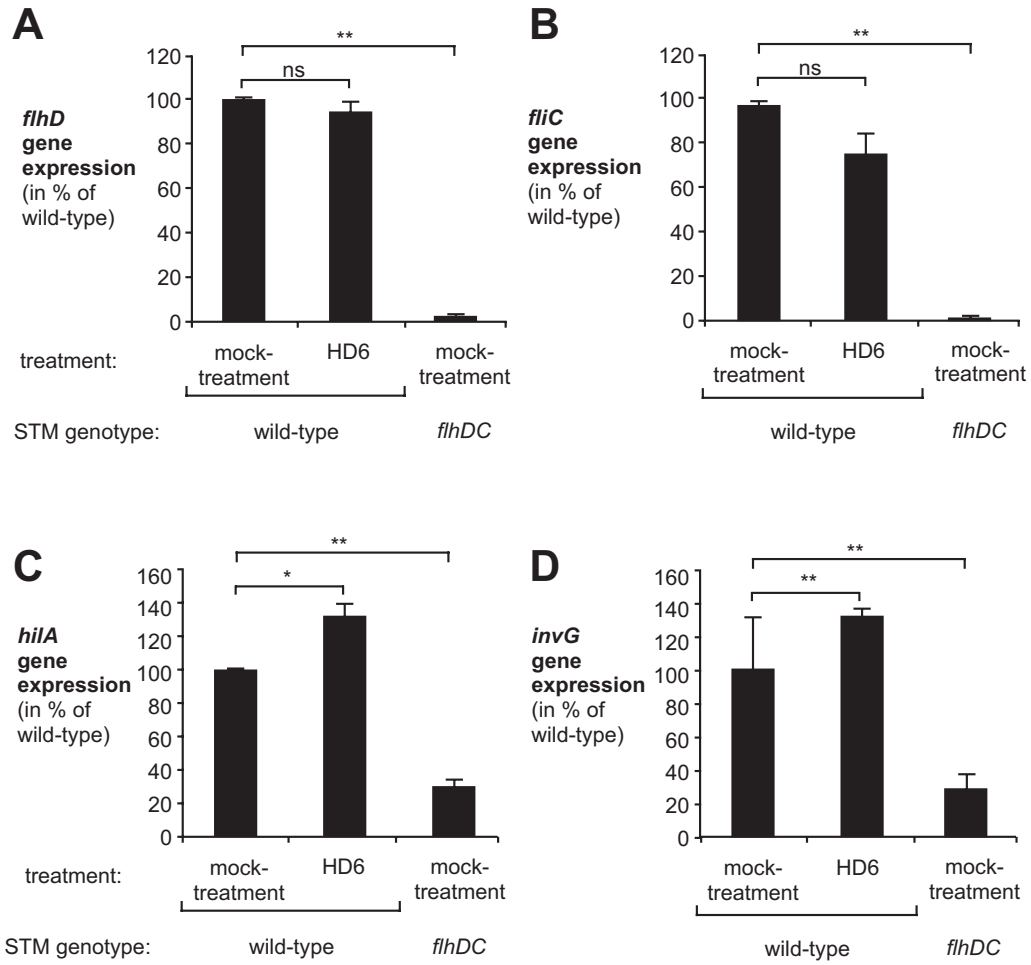

Fig. S6. Analysis of *S.* Typhimurium gene expression upon treatment with HD6.

RT-PCR analysis of (A) *flhD*, (B) *fliC*, (C) *hilA* and (D) *invG* gene expression following HD6-treatment, relative to mock (vehicle alone)-treated wild-type *S.* Typhimurium (STM). The *flhD* gene encodes for a subunit of the flagellar master regulator FlhDC, an activator of the flagellar regulon, which includes the *Salmonella* pathogenicity island (SPI)-1 T3SS regulator *fliZ*. The *fliC* gene encodes the phase 1 flagellin FliC. The *hilA* gene encodes HilA, a key SPI-1 activator, and the *invG* gene encodes a structural protein of the T3SS-1 complex. Mock-treated *flhDC* deletion mutant *S.* Typhimurium served the control for each experiment. Error bars represent SEM. **P* < 0.05, ***P* < 0.01, *t*-test on ln-transformed data. Data are representative of three experiments.

Fig. S7

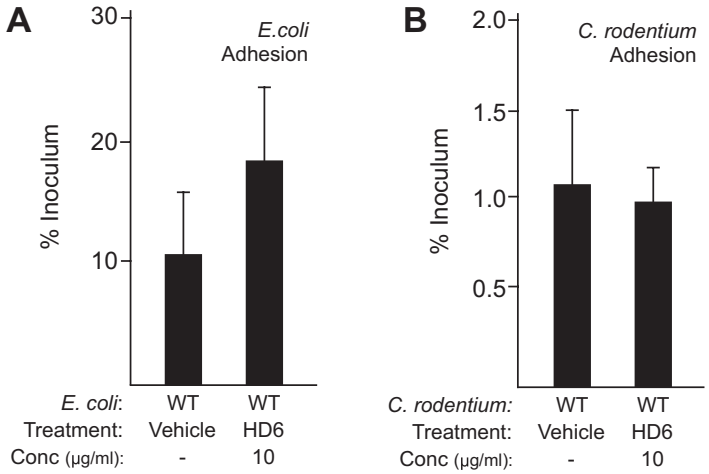

Fig. S7. Analysis of HD6 effects on bacterial adhesion to intestinal epithelial cells.

In vitro bacterial adhesion assay using colonic T84 cells. (A) *E. coli* or (B) *C. rodentium* (1 x 10^6 CFU) were treated for 30 min with HD6 (10 µg/ml) or vehicle control. The epithelial cells were then incubated with the bacteria for 1 h at 37ºC (MOI of 10). The media was aspirated, the epithelial cells were washed with PBS, and then epithelial cells were lysed with 0.05% Triton X-100. Bacterial numbers were determined by plating and counting colonies. Data are representative of four (A) or three (B) independent experiments. Error bars represent SEM.

Fig. S8

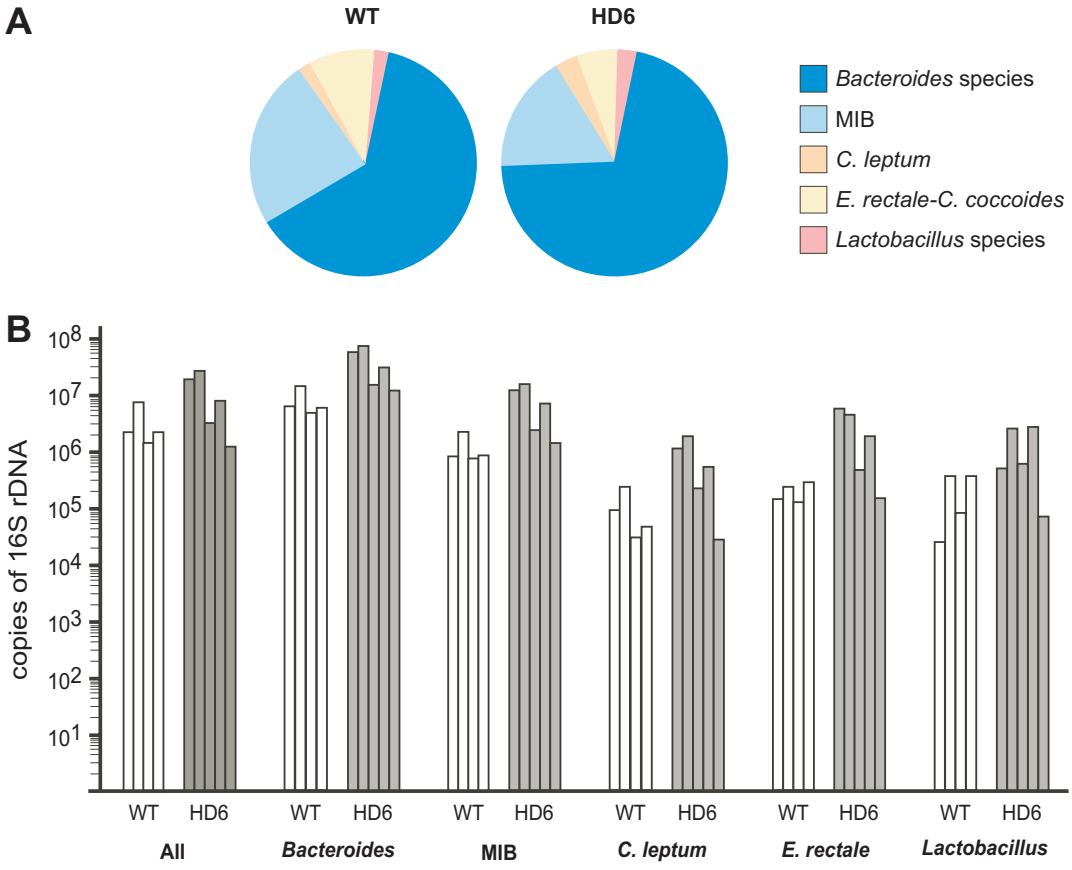

Fig. S8. Quantitative real-time PCR analysis of fecal microbiota in HD6 and wild-type littermates.

DNA was isolated from fecal pellets from the distal colon of 6-week wild-type and hemizygous (+/-) HD6 transgenic littermates. Specimens were analyzed by quantitative real-time PCR using group specific 16S rDNA primers as described (*9*). (A) Pie graph show averages for each bacterial group for the two mouse genotypes. (B) Bar graphs show data for individual wild-type (white bars, n=4) and HD6 transgenic (gray bars, n=5) mice. Data are representative of two independent experiments.

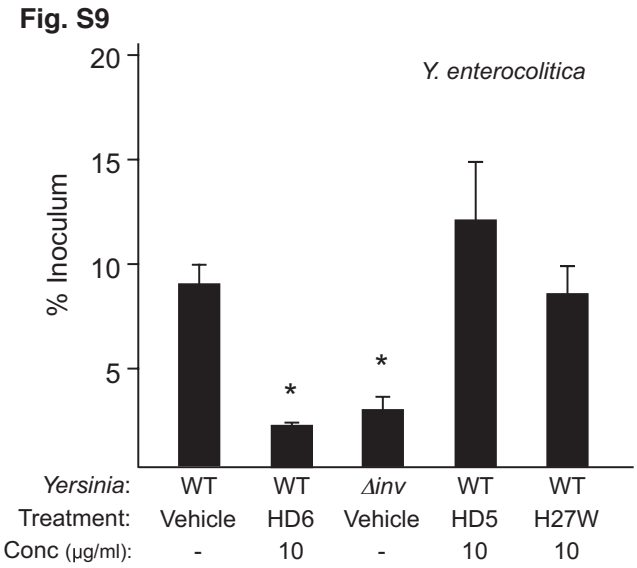

Fig. S9. *In vitro* invasion assay of HD6-treated *Y. enterocolitica.*

In vitro invasion assay of wild-type *Y. enterocolitica* using epithelial T84 cells. *Y. enterocolitica* (GY123) were pre-treated for 1 h with 10 μg/ml of either HD6, HD5, or H27W-HD6, or with vehicle alone. The Δ*inv* mutant (GY5583) was treated with vehicle alone. Bacteria were then allowed to invade the epithelial cells (MOI of 10) for 1 h. Cells were then washed, treated with gentamicin, and then lysed to quantitate intracellular bacteria (expressed as % of initial inoculum). The data averages of three experiments and are representative of 3 independent experiments. Error bars are SEM. **P* < 0.01, *t*- test.

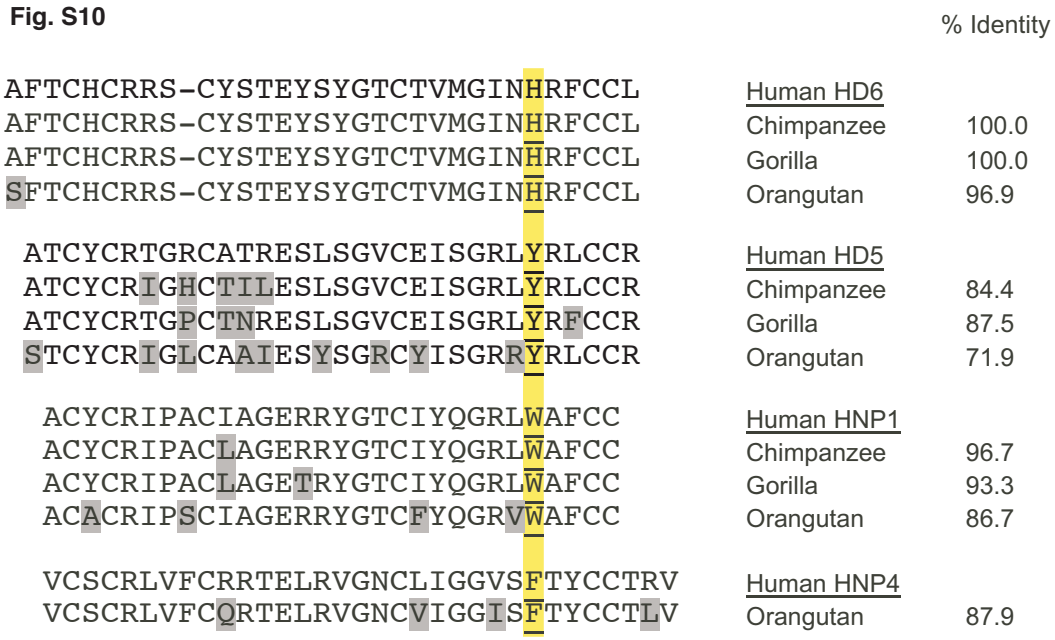

Fig. S10 Amino acid sequence alignment of hominid α-defensins.

Amino acid sequence of the mature human HD6, HD5, HNP1, and HNP4 are compared to their orthologs from other hominids. Note that HNP2 and HNP3 differ from HNP1 solely at N-terminal residue (*1*). Gray boxes indicate non-identity compared with the human sequences. Yellow shading and underline highlight amino acid residues corresponding to position 27 of HD6.

Fig. S11

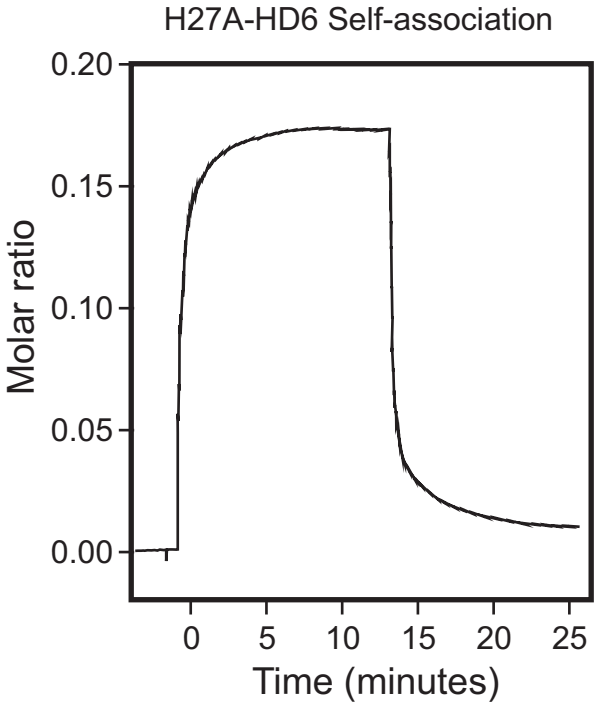

Fig. S11 Surface plasmon resonance (SPR) analysis of H27A-HD6 self-association.

The SPR biosensor presented 511 resonance units (RU) H27A-HD6. H27A-HD6 (5 μg/ml) in HBS-EP buffer and traversed the biosensor at 50 μl/min. The molar ratio calculation, which takes into account the relative masses of the analyte and ligand and the number of RU presented by the biosensor, is described in the methods. Shown are representative data from at least three separate experiments.

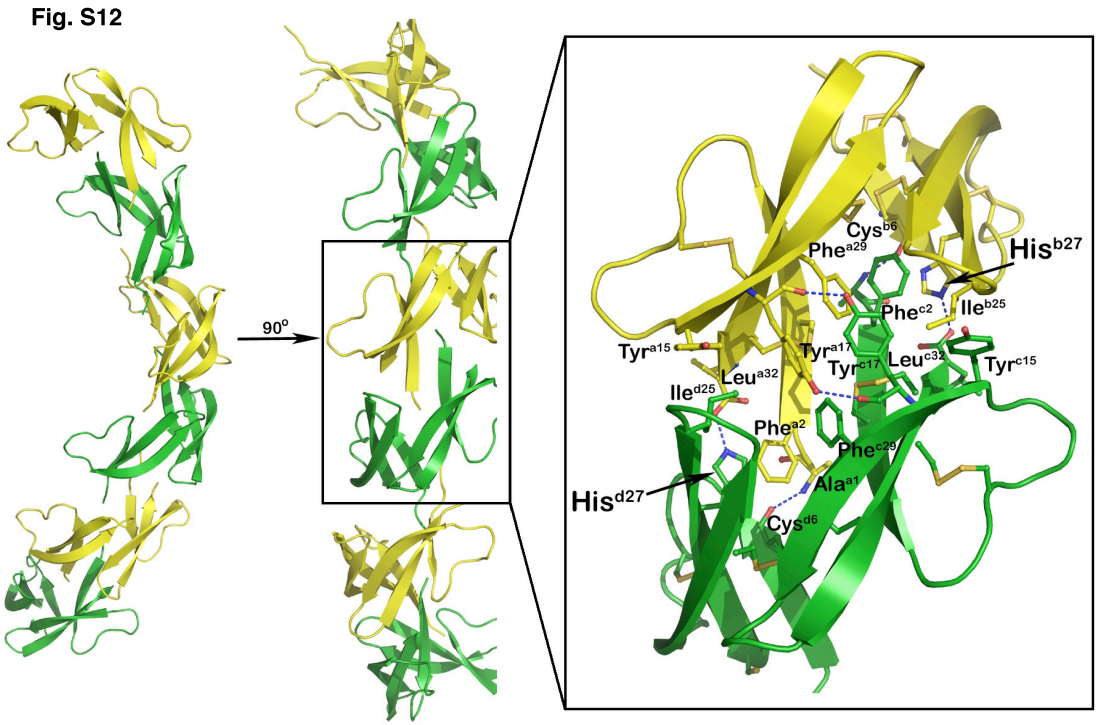

Fig. S12. Oligomeric state of HD6 in the crystal.

Quaternary structure of wild-type HD6 in the crystal (left) and close-up view of the tetramer interface (right) (PDB code 1ZMQ) (*15*). 'Canonical' dimers are colored yellow and green, which form a tetramer through β1 strand-mediated dimer-dimer interactions. Contiguous tetramers can potentially form an elongated helical structure as previously suggested (*15*). Residues involved in tetramer formation are shown as ball-and-sticks in the close-up view of the tetramer interface. The hydrophobic core of the tetramer primarily comprises the side chains of Phe2, Tyr17, Phe29 and the Cys4-Cys31 disulfide, and is further supported by hydrophobic stacking between Tyr15 and Ile25. Hydrogen bonds involving His27-Leu32, Ala1-Cys6 and Tyr17-Tyr17 pairs are represented by blue dashes; inter-strand main-chain hydrogen bonds that stabilize dimer and tetramer are omitted here and shown in Fig. 3A.

Fig. S13

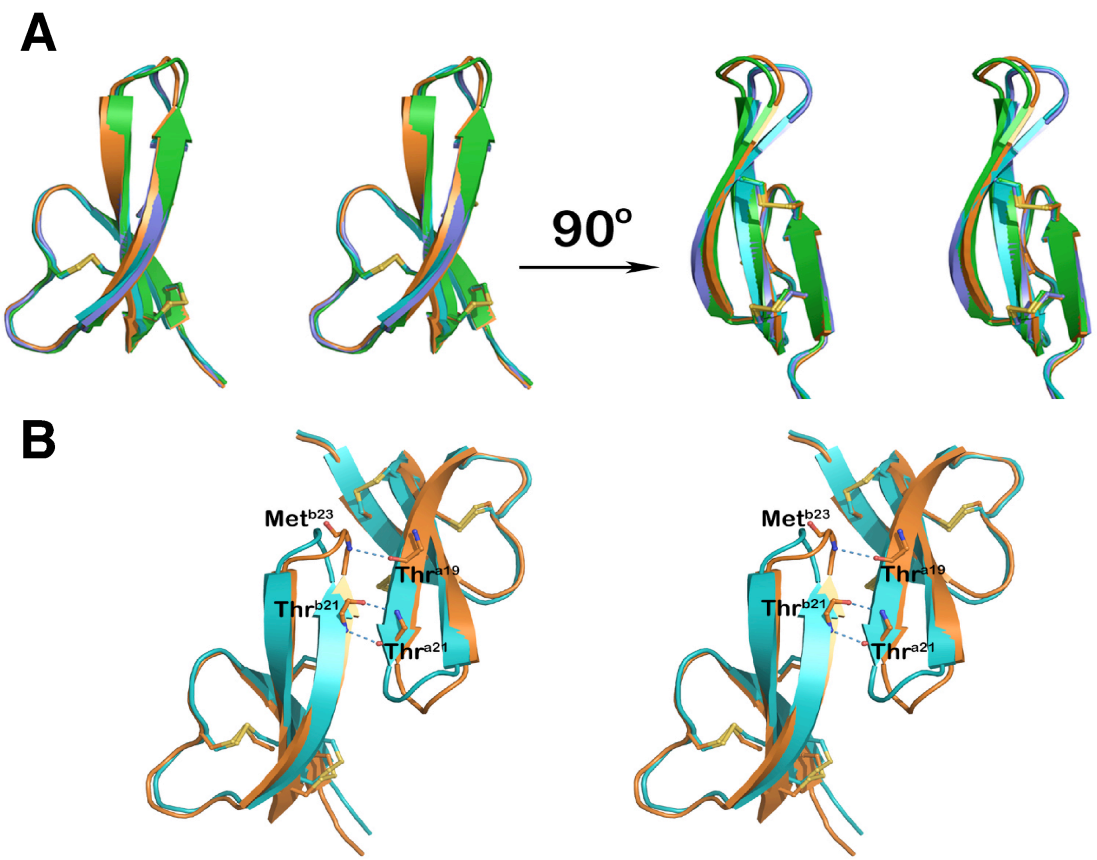

Fig. S13. Crystal structure of H27W-HD6.

Stereo view of four superimposed monomers present in the asymmetric unit of monoclinic crystal. (A) Disulfide bonds are shown as ball-and-sticks, whereas Cα-traces are shown as ribbons. The overall fold is very well defined and conserved among all monomers present in the asymmetric unit with some conformational flexibility restricted to the β2-hairpin region. Pairwise superposition of Cα atoms resulted in RMSDs in the range of 0.3-0.9 Å for 32 residues. (B) Stereo view of superimposed Cα-traces of two crystallographically independent 'canonical' dimers of H27W-HD6. One dimer is formed within the asymmetric unit, and the other by symmetry-related copies. Dimerization is mediated primarily through the hydrogen bonds between the backbone atoms of the β2 strands. Formation of these weakly associated dimers results in the burial of an average of 220 $Å^2$ of molecular surface per monomer.

Fig. S14

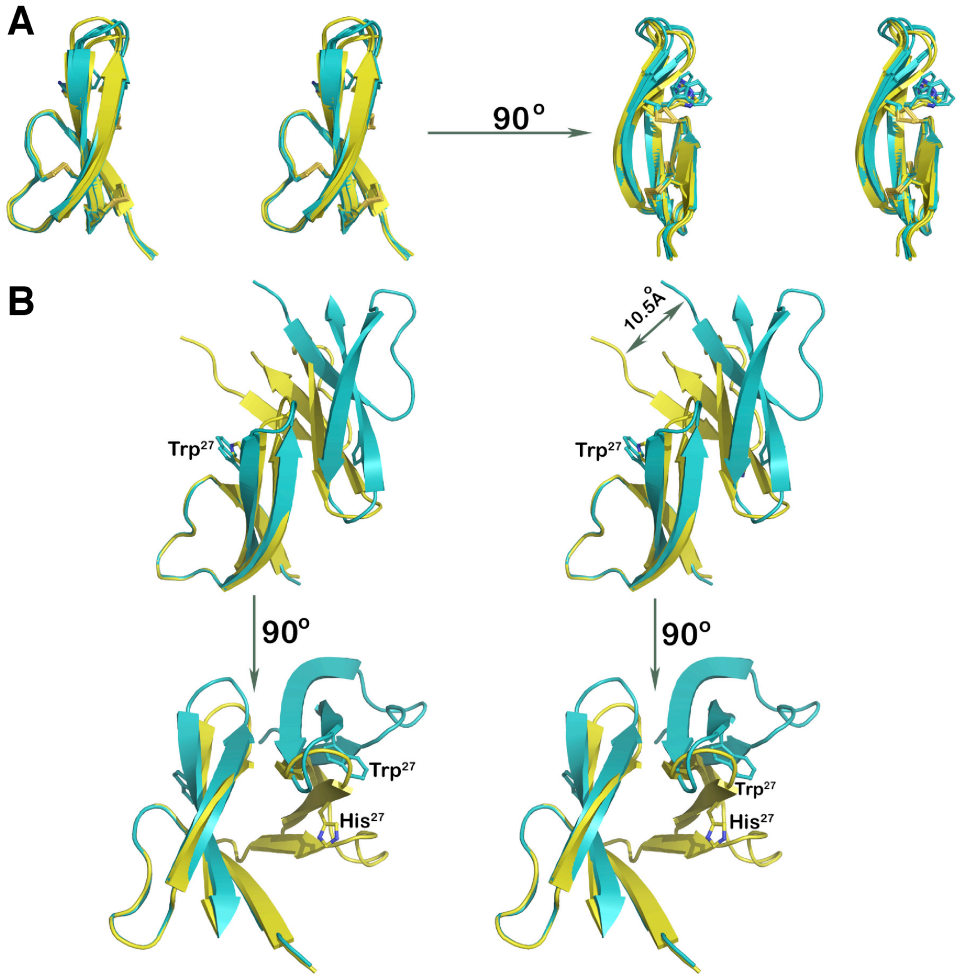

Fig. S14. Comparison of HD6 and H27W-HD6 crystal structures.

(A) Stereo view of eight superimposed, crystallographically independent monomers of H27W-HD6 (cyan) and HD6 (yellow). Disulfide bonds and the side chains of Trp27 and His27 are shown as ball-and-sticks, whereas Cα-traces are shown as ribbons. Superposition of monomers shows an extensive structural conservation of Cα atoms with minor fluctuations in the β2-hairpin region in both HD6 and H27W-HD6. Pairwise superposition of Cα atoms resulted in RMSDs in the range of 0.7-1.1 Å for 32 residues. (B) Stereo view of superimposed 'canonical' dimers. In contrast to the slightly twisted dimer interface of HD6 (yellow), the dimer interface of H27W-HD6 (cyan) is rather flat with both β2 strands lying approximately in the same plane. The twist propagates along the β1 and β3 strands and induces inter-monomer stabilizing contacts between the side chains of Cys3 and Cys31 in HD6. Such interactions are limited in H27W-HD6 dimers. Consequently, 20% more molecular surface area is buried in HD6 dimers than in H27W-HD6 dimers.

Fig. S15

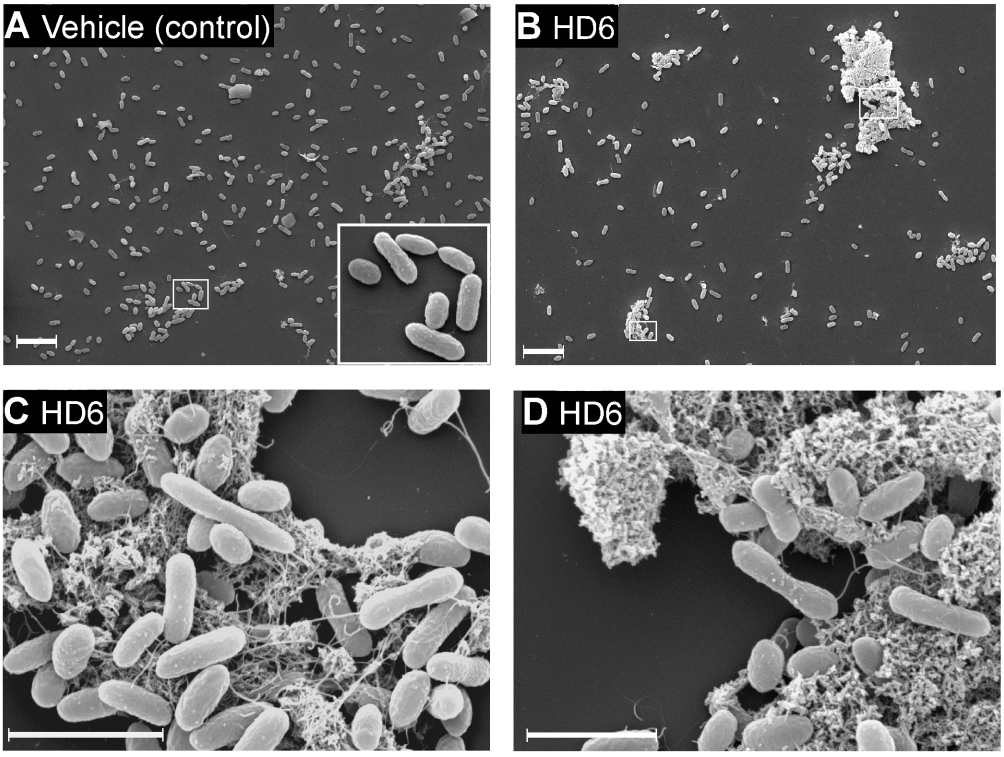

Fig. S15. HD6 nanonets entangles *S.* Typhimurium in human ileal fluid.

Scanning electron microscopy of wild-type *S.* Typhimurium treated with either vehicle (A) or HD6 (10 μg/ml, (B-D)) in clarified human small intestinal aspirate. See methods for details. Bar = 5 μm. Data are representative of 6 experiments.

Fig. S16

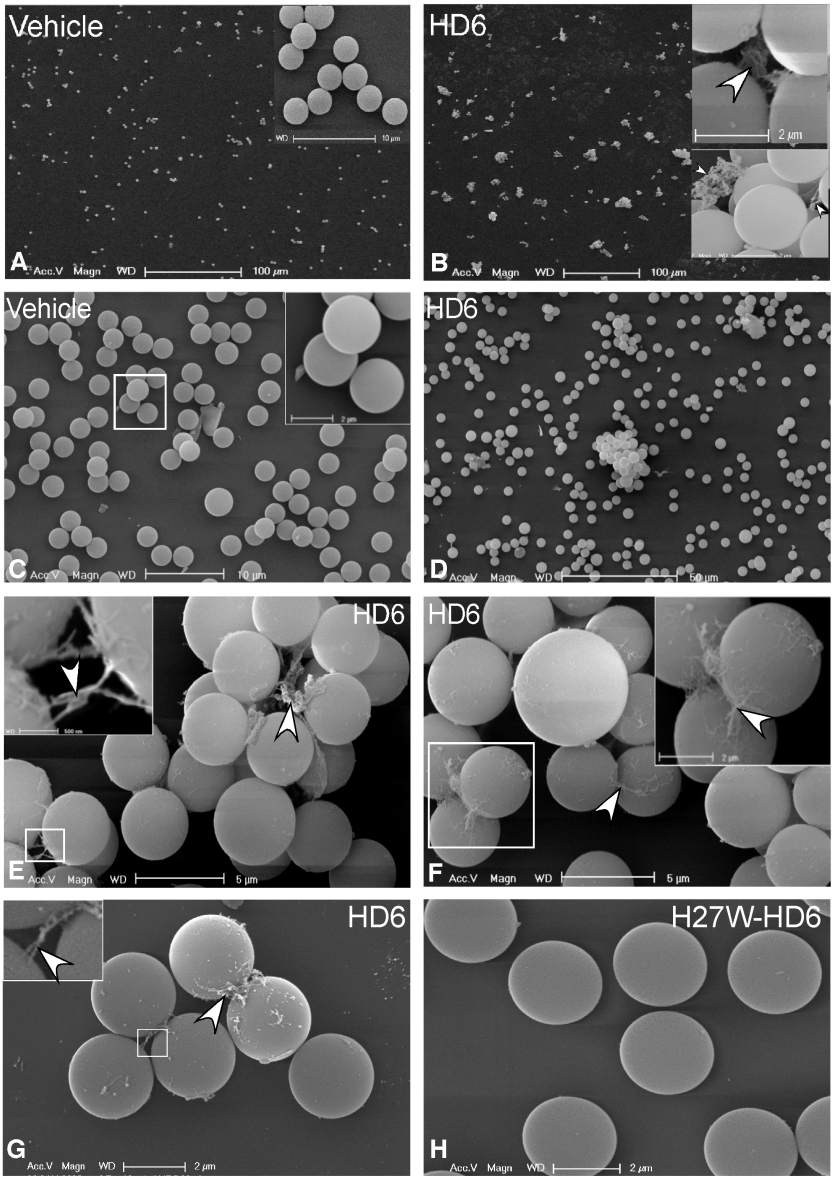

Fig. S16. HD6 aggregates protein-coated polystyrene beads via nanonet formation.

Scanning electron microscopy images of polystyrene beads, coated by covalent attachment of *Salmonella* type I fimbriae (A-B) or protein A (C-H). Beads were incubated in 50 mM Tris-maleate buffer at room temperature with 1 μg/ml HD6 for 5 min (B, C-F), 10 μg/ml HD6 for 30 min (G), 10 μg/ml H27W-HD6 for 30 min (H) or with buffer alone (vehicle, A, D). The beads were then washed, fixed overnight, and processed for SEM. Arrowhead indicates HD6 nanonets aggregating beads coated with type I fimbrial proteins (B) and protein-A (E-G). No similar structures were observed with H27W-HD6 (H) or if HD6 peptide was omitted (A, C). Data are representative of at least two independent experiments.

Fig. S17

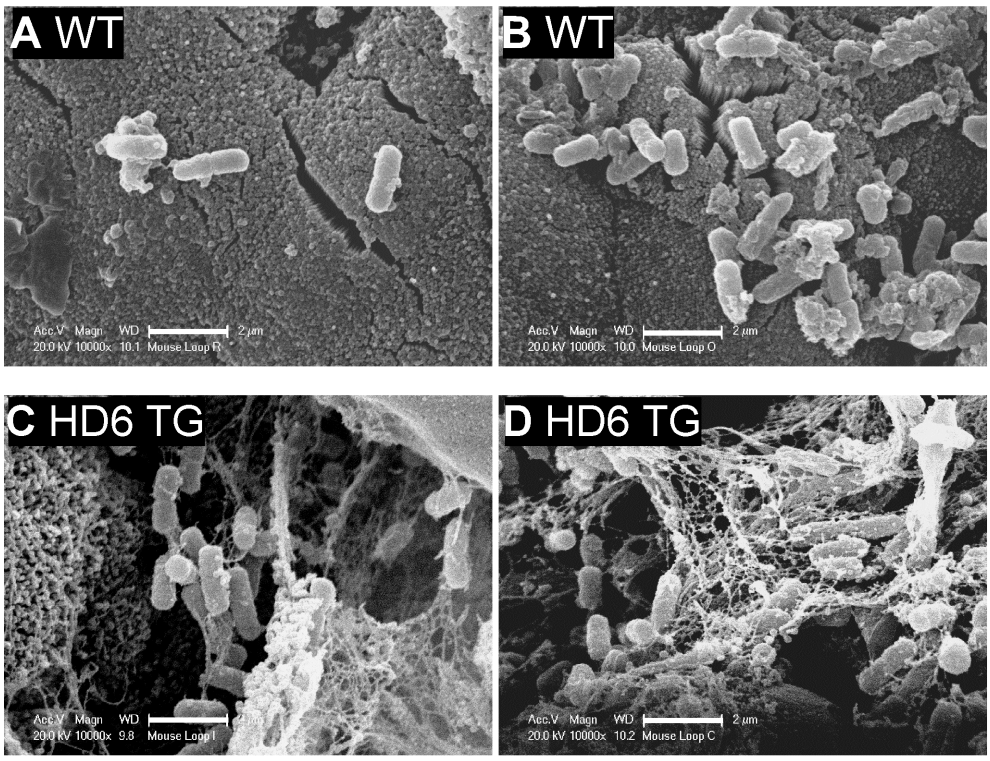

Fig. S17. HD6 nanonets entrap *S.* Typhimurium *in vivo*.

SEM of wild-type (A, B) and HD6 transgenic (C, D) mouse ileal loop directly inoculated with *S.* Typhimurium. These four images, together with the four shown in Fig. 4B were among a total of 12 obtained in a double-blinded data acquisition and scoring evaluation, where three individuals scored all images correctly for mouse genotype. ** $P < 0.001$, Fisher's exact test. Data are representative of two independent experiments. See methods for details. Bar = 2 μm.

Fig. S18

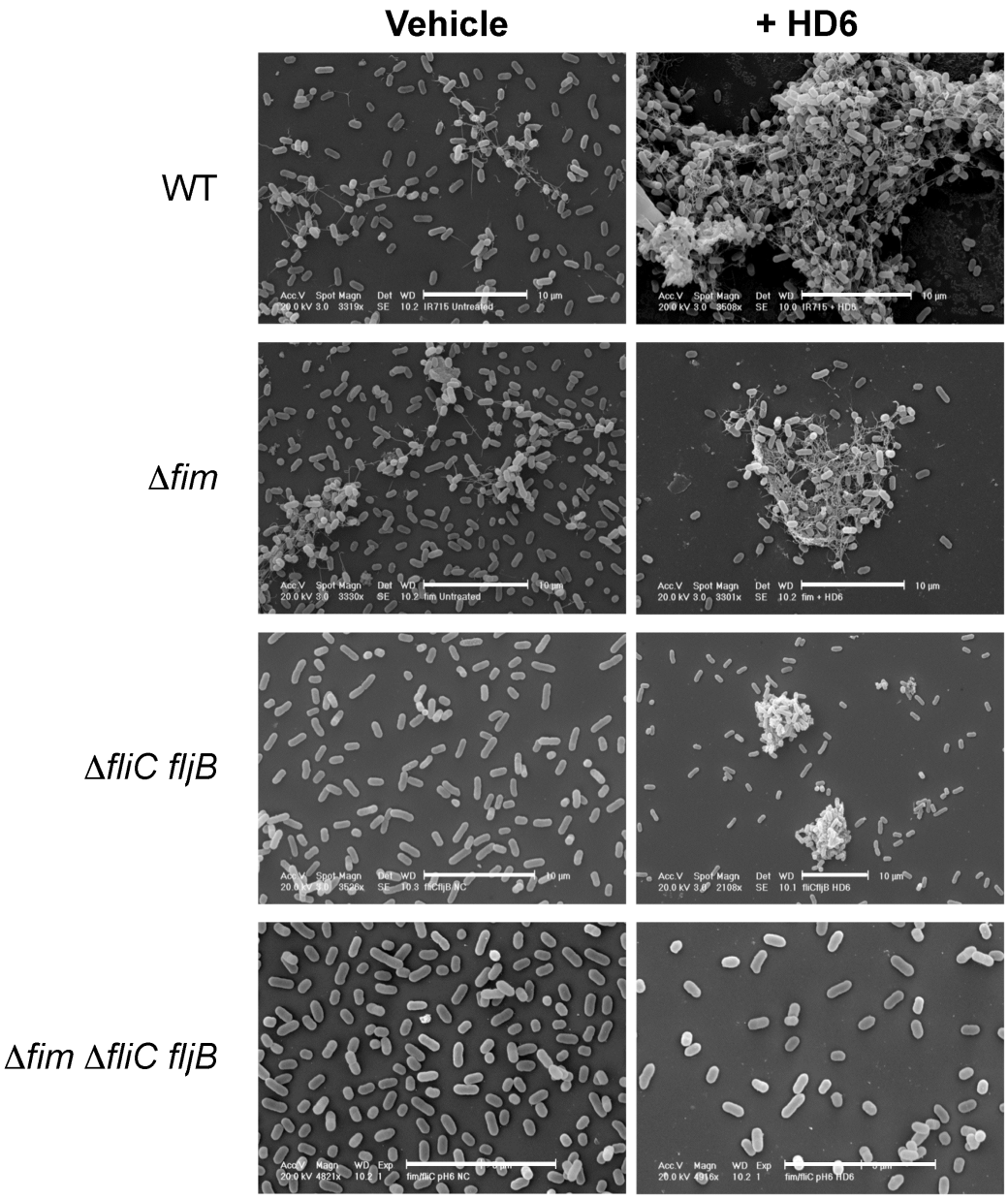

Fig. S18. *S.* Typhimurium flagella and fimbriae are bacterial targets for HD6 binding for nanonet formation.

Scanning electron microscopy of IR715 wild-type *S.* Typhimurium, Δ*fim*, and Δ*fliC fljB* treated with vehicle alone (top row) or 10 μg/ml HD6 (bottom row). While nanonets and aggregation with HD6 are decreased in the single flagellin and fimbrin deficient mutants (shown here), the last arm of the experiment with the double mutant (Δ*fim* Δ*fliC fljB*) is shown in Fig. 4C. Data are representative of three independent experiments. See methods for details. Bar = 10 μm.

Table S1. Bacterial Strain Table

Strain	Relevant genotype	Reference
Salmonella enterica serovar Typhimurium		
IR715	ATCC 14028, Nal^R derivative	(*31*)
EHW2	IR715 Δ*fimAICDHF*(+40 to +5970)::KSAC	(*32*)
SPN313	IR715 Δ*fliC*(-25 to +1494) *fljB5001*::Mu*d*Cm	(*29*)
SPN449	IR715 Δ*invA*(-9 to +2057)::*tetRA*	(*33*)
SPN494	IR715 Δ*fliC*(-25 to +1494) *fljB5001*::Mu*d*Cm Δ*fimAICDHF*(+40 to +5970)::KSAC	This work
SW258	IR715 P(*flhDC*)5451::T-POP	PMID 19451244
Y. enterocolitica		
GY123	WT Serotype O:8	
GY5583	Serotype 0:8, *inv*	
C. rodentium		
DBS100	ATCC 51459	
E. coli		
CDCB6914-MS1	ATCC: 43888, Serotype 0157:H7	

Table S2. Data collection and refinement statistics

Data collection	
Wavelength, Å	1.54
Space group	$P2_1$
Cell parameters	
a, b, c, Å	33.8, 32.7, 54.0
α, β, γ, °	90, 108.4, 90
Molecules/a.u.	4
Resolution, (Å)	50-1.95 (1.98-1.95)
Number of reflections	
Total	15,714
Unique	8,258
R_{merg}[b], %	10.5 (57.9)
I/σ	16.5
Completeness, %	99.2 (92.0)
Redundancy	5.7 (4.7)
Refinement Statistics	
Resolution, Å	20-1.95
R[c], %	19.2
R_{free}[d], %	24.5
Number of atoms	
Protein	1,036
Water	41
Ligand/Ion	3
Root mean square deviation	
Bond lengths, Å	0.018
Bond angles, °	1.8
Ramachandran	
favored, %	99.2
allowed, %	0.8
outliers, %	0.0

Values in parentheses are for highest-resolution shell

[b] $R_{merge} = \sum | I - \langle I \rangle | / \sum I$, where I is the observed intensity and $\langle I \rangle$ is the average intensity obtained from multiple observations of symmetry-related reflections after rejections

[c] $R = \sum \| F_o | - | F_c \| / \sum | F_o |$, where F_o and F_c are the observed and calculated structure factors, respectively

[d] R_{free} = defined by Brünger (*34*)